Published online 22 February 2012 *Nucleic Acids Research, 2012, Vol. 40, No. 11* ***4965–4976***
doi:10.1093/nar/gks167

The asparagine-transamidosome from *Helicobacter pylori*: a dual-kinetic mode in non-discriminating aspartyl-tRNA synthetase safeguards the genetic code

Frédéric Fischer[1], Jonathan L. Huot[2], Bernard Lorber[1], Guillaume Diss[1], Tamara L. Hendrickson[3], Hubert D. Becker[1], Jacques Lapointe[2,*] and Daniel Kern[1,*]

[1]Institut de Biologie Moléculaire et Cellulaire, UPR 9002 du CNRS, Architecture et Réactivité de l'ARN, Université de Strasbourg, 15 rue René Descartes, 67084 Strasbourg Cedex, France, [2]Département de Biochimie, de Microbiologie et de Bio-informatique, PROTEO, Université Laval, 1045 av. de la Médecine, Québec (Québec), Canada G1V 0A6 and [3]Department of Chemistry, Wayne State University, 5101 Cass Ave, Detroit, MI 48202, USA

Received November 1, 2011; Revised January 31, 2012; Accepted February 1, 2012

ABSTRACT

Helicobacter pylori **catalyzes Asn-tRNA^{Asn} formation by use of the indirect pathway that involves charging of Asp onto tRNA^{Asn} by a non-discriminating aspartyl-tRNA synthetase (ND-AspRS), followed by conversion of the mischarged Asp into Asn by the GatCAB amidotransferase. We show that the partners of asparaginylation assemble into a dynamic Asn-transamidosome, which uses a different strategy than the Gln-transamidosome to prevent the release of the mischarged aminoacyl-tRNA intermediate. The complex is described by gel-filtration, dynamic light scattering and kinetic measurements. Two strategies for asparaginylation are shown: (i) tRNA^{Asn} binds GatCAB first, allowing aminoacylation and immediate transamidation once ND-AspRS joins the complex; (ii) tRNA^{Asn} is bound by ND-AspRS which releases the Asp-tRNA^{Asn} product much slower than the cognate Asp-tRNA^{Asp}; this kinetic peculiarity allows GatCAB to bind and transamidate Asp-tRNA^{Asn} before its release by the ND-AspRS. These results are discussed in the context of the interrelation between the Asn and Gln-transamidosomes which use the same GatCAB in *H. pylori*, and shed light on a kinetic mechanism that ensures faithful codon reassignment for Asn.**

INTRODUCTION

Accurate expression of genetic information is essential to all living organisms. Integrity of the message encoded within a gene is safeguarded by mechanisms that cells have evolved at each step of gene expression. In protein synthesis, tRNA aminoacylation is a crucial step where each tRNA species is bound to its cognate amino acid in reactions catalyzed by the aminoacyl-tRNA synthetases (aaRSs) (1,2). The amino acids are first activated as aminoacyl∼AMPs and then transferred onto their cognate tRNAs to synthesize the final aminoacyl-tRNA products. The latter are then carried to the ribosome by an elongation factor where they are used to decode the codons on the mRNA. Fidelity of translation depends on accurate tRNA aminoacylation, i.e. correct matching of an amino acid to its set of isoacceptor tRNAs. This coupling is determined by the existence of a particular aaRS for each amino acid/tRNA pair. The capacity to select homologous substrates is conferred by active site geometry and by correction processes that are used by aaRSs when the wrong aminoacyl-tRNAs are formed

*To whom correspondence should be addressed. Tel: +33 3 88 41 70 92; Fax: +33 3 88 60 22 18; Email: d.kern@ibmc-cnrs.unistra.fr
Correspondence may also be addressed to Jacques Lapointe. Tel: +1 418 656 2131 (Extn 3411); Fax: +1 418 656 3664; Email: jacques.lapointe@bcm.ulaval.ca

The authors wish it to be known that, in their opinion, the first two authors should be regarded as joint First Authors.

(3,4). Moreover, aaRSs are split into two classes, according to sequence/structure (5) and kinetic (6–8) properties. Members of class I bind tRNA on the minor grove side and acylate the 2′-OH of the terminal adenosine whereas the members of class II approach tRNA from the major grove side and transfer the amino acid moiety on the 3′-OH of the terminal adenosine. Further, it seems that most class I aaRSs display a rate-limiting step for the release of aminoacyl-tRNA, whereas the transfer of the activated amino acid onto tRNA is rate-limiting for class II aaRSs (8).

Global genome analyses and biochemical data indicate that about half of prokaryotes are deprived of asparaginyl-tRNA synthetase (AsnRS), and that the vast majority lack a glutaminyl-tRNA synthetase (GlnRS). This pattern negates the old 'dogma' that postulated the presence of a specific aaRS for each amino acid and tRNA pair (9,10). These organisms, including mitochondria (11), all synthesize amidated aminoacyl-tRNAs thanks to an enzymatic system that includes a non-discriminating (ND) aaRS, ND-aspartyl-tRNA synthetase (ND-AspRS) and/or ND-glutamyl-tRNA synthetase (ND-GluRS), providing a misacylated aminoacyl-tRNA species (Asp-tRNA^{Asn} or Glu-tRNA^{Gln}); these aminoacyl-tRNAs are then modified into Asn-tRNA^{Asn} or Gln-tRNA^{Gln} through a phosphorylation/transamidation mechanism catalyzed by a tRNA-dependent amidotransferase called GatCAB in bacteria (12–20). The synthesis of Asn-tRNA^{Asn} and Gln-tRNA^{Gln} is ensured by two separate bi-enzymatic systems, consisting in functionally related enzymes brought together by a scaffold/substrate tRNA. The resulting aaRS/tRNA/GatCAB complexes are named transamidosomes. These particles vary in cohesive strength, with the Asn-transamidosome of *Thermus thermophilus* (21) showing the highest stability while the Gln-transamidosomes of *Thermotoga maritima* and *Helicobacter pylori* are more dynamic (22–24). Within all of these complexes, the tRNA moiety can be used either as a scaffold for the nucleoprotein to form Asn or Gln or as a substrate for their synthesis. This makes the misacylation/transamidation system a matrix-assisted amino acid biosynthesis pathway of particular interest in *H. pylori*, a well-known and widespread human pathogen, which uses these indirect pathways to form Asn, Gln-tRNA^{Gln} and Asn-tRNA^{Asn} (24–28).

Although it was shown that mischarged Asp-tRNA^{Asn} and Glu-tRNA^{Gln} species are deprived of significant affinity for the elongation factor EF-Tu (29,30), several investigations have shown that they can lead *in vivo* to incorporation of Asp (31,32) or Glu (33–35) in place of Asn and Gln into proteins. Overexpression of either misacylating aaRS is toxic in *Escherichia coli* (31–35) while in yeast a disabled amidotransferase resulted in significant incorporation of Glu at Gln codons in mitochondrial proteins (36). Asn- and Gln-transamidosomes, which control the release of misacylated intermediates, may therefore be another layer of aminoacyl-tRNA quality control.

Here, we report how this quality control is achieved for Asn-tRNA^{Asn} synthesis in *H. pylori* through the formation of an Asn-transamidosome. Moreover, we show that ND-AspRS exhibits surprisingly sensitive kinetic properties for Asp-tRNA^{Asp} and Asp-tRNA^{Asn} formation: fast release of Asp-tRNA^{Asp} for translation and slow release of Asp-tRNA^{Asn} to allow transamidosome formation by GatCAB binding. This safeguard mechanism resembles an editing process and may shed light on evolutionary processes that led to Asn infiltration into the present-day genetic code. Our results suggest that, in *H. pylori*, ND-AspRS and GatCAB co-evolved to generate an appropriate kinetic system able to reduce translational error level and to ensure a faithful codon reassignment for Asn.

MATERIALS AND METHODS

Overproduction and purification of enzymes and tRNAs

The *H. pylori* (*Hp*) ND-AspRS and GatCAB were overproduced from the cloned *aspS, gatC, gatA* and *gatB* genes as described (28,32). For protein purification, the cells from an overnight culture were harvested by centrifugation at 4000*g*, washed in cold Tris–HCl buffer 100 mM, pH 8.0, sedimented and suspended in the cell disruption buffer (1/3, w/v) formed by supplementing the above buffer with 5 mM 2-mercaptoethanol, 0.1 mM Na_2EDTA, 1 mM benzamidine and 1 mM of protease inhibitors [4-(2-aminoethyl)-benzenesulfonyl fluoride hydrochloride, AEBSF, Pefablock]. The cell extract, obtained by sonication of the cell suspension and centrifugation at 105 000*g*, was dialyzed against potassium phosphate buffer 20 mM, pH 7.2, containing 0.5 mM Na_2EDTA and 5 mM 2-mercaptoethanol, and adsorbed on a DEAE-cellulose column followed by elution with a linear gradient of potassium phosphate from 25 to 250 mM pH 7.2.

The AspRS-containing fractions, eluted between 130 and 150 mM salt, were then adsorbed on a Ni-NTA column in 50 mM Tris–HCl buffer pH 7.5 before elution of the proteins with a linear gradient from 25 to 450 mM of imidazole. Pure AspRS (10 mg at 95% purity) were obtained from 30 g cells. The GatCAB containing fractions eluted on DEAE-cellulose from 160 to 190 mM potassium phosphate were adsorbed on a Ni-NTA column in 50 mM Tris–HCl buffer pH 7.5. After washing with the buffer containing 25 mM imidazole, GatCAB was eluted with 450 mM imidazole. Pure GatCAB (50 mg at 95% purity) was obtained from 80 g of cells.

The reconstituted tRNA^{Asn} gene from *T. thermophilus* was cloned in the pKK223 vector and purified as described (21). The *E. coli* (*Ec*) tRNA^{Asp} gene was amplified from genomic DNA and cloned into the pUC18 vector for expression in the *E. coli* JM103 strain. Transfer RNA^{Asp} (800 mg from 120 g of cells; accepting capacity 30.6 nmol.mg^{-1}) was obtained by phenol extractions followed by chromatographies on DEAE-cellulose and nmol.mg Sepharose 4B as described (37). All tRNA^{Asp} and tRNA^{Asn} mutants used in this study were cloned into the pUC18 vector downstream a T7 promoter, transcribed and purified as described (38).

Gel-filtration

Experiments were conducted as described (21) using an ÄKTA Purifier and a 24-ml Superdex G200 column (GE Healthcare) equilibrated with 50 mM Na–HEPES buffer pH 7.2 containing 30 mM KCl, 6 mM $MgCl_2$, 0.1 mM Na_2EDTA and 5 mM 2-mercaptoethanol at 12°C. Samples of 0.2 ml containing the enzyme and tRNA partners at the indicated concentrations were diluted in the equilibration buffer and analyzed. K_D values [free enzyme] × [free $tRNA^{Asn}$]/[enzyme/$tRNA^{Asn}$ complex] were determined by evaluation of the areas of enzyme-bound tRNA and free tRNA peaks, the sum of which equals the total tRNA present in the sample. The contaminating non-specific tRNA was subtracted from free tRNA. The quantity of free enzyme was determined by subtracting the quantity of enzyme-bound tRNA from total amount of enzyme in the sample.

Dynamic light scattering

Dynamic light scattering (DLS) experiments were conducted as described (21) at 20 ± 0.1°C in a Zetasizer NanoS instrument (Malvern, UK). The 20- to 40-µl samples contained 10 µM ND-AspRS (20 µM subunits) and/or 20 µM GatCAB with or without 20 µM $tRNA^{Asn}$ in the gel-filtration buffer. When present, ATP, Asp and Gln were at a concentration of 2 mM. Hydrodynamic diameters were corrected for solvent refractive index (n = 1.3353) and absolute viscosity (η = 1.041 mPa.s).

Aminoacylation of tRNA

The reaction mixture contained 100 mM Na–HEPES buffer pH 7.2, 30 mM KCl, 12 mM $MgCl_2$, 2 mM ATP, 20–50 µM [^{14}C] L-Asp (330 cpm.pmol^{-1}, GE Healthcare), 0.1 mg.ml^{-1} bovine serum albumin, 10 µM *T. thermophilus* (*Tt*) $tRNA^{Asn}$ or *Ec* $tRNA^{Asp}$, or 0.04–6 µM *Tt* $tRNA^{Asn}$ for K_M measurements, and 0.01–0.5 µM *Hp* ND-AspRS. The reactions were conducted at 37°C unless otherwise indicated. The rate-limiting step was determined with 0.5, 1.0 and 1.5 µM *Hp* ND-AspRS and 10 µM $tRNA^{Asn}$ or $tRNA^{Asp}$ without or with GatCAB at the indicated concentrations in the presence of 15% glycerol at 4°C. For K_M measurements of Asp and ATP in the presence of $tRNA^{Asp}$ or $tRNA^{Asn}$, the small substrate concentrations varied from 10 to 300 µM and tRNA was present at a 10 µM concentration. Inhibition experiments with aspartol-adenylate (Asp-ol-AMP), kindly provided by Prof. R. Chênevert (Université Laval, Québec), were performed with concentrations ranging from 10 to 200 µM. The inhibition constants were determined as described (39). The [^{14}C] aminoacyl-tRNA formed in 10 or 20 µl aliquots withdrawn at various time intervals was determined as described (1).

ATP-PPi exchange

The reaction mixture contained 100 mM Na–HEPES buffer pH 7.2, 10 mM $MgCl_2$, 2 mM L-Asp, 2 mM ATP, 2 mM [^{32}P] PPi (2 cpm.pmol^{-1}, Perkin Elmer) and 0.5 µM ND-AspRS. The [^{32}P] ATP formed at 37°C was determined in 40 µl aliquots at various time intervals as described (1).

Transamidation of Asp-$tRNA^{Asn}$

Reactions were conducted at 37°C for 10 min in a mixture containing 100 mM Na–HEPES buffer pH 7.2, 30 mM KCl, 12 mM $MgCl_2$, 2 mM ATP, 10 µM [^{14}C] L-Asp (330 cpm.pmol^{-1}), 1 mM L-Gln, 0.1 mg.ml^{-1} bovine serum albumin and 10 µl of the transamidosome fraction eluted from size-exclusion chromatography. Transamidation was measured as described (21,24).

RESULTS

An Asn-transamidosome in *H. pylori*

Association of ND-AspRS, $tRNA^{Asn}$ and GatCAB from *T. thermophilus* leads to a stable ternary complex named Asn-transamidosome (21). Gel-filtration and DLS experiments conducted with the *H. pylori* partners show that the ND-AspRS can bind both $tRNA^{Asp}$ and $tRNA^{Asn}$ but with different affinities (K_D values of 7.9 and 21.4 µM respectively, Figure 1A) and that GatCAB can form a much more stable binary complex with $tRNA^{Asn}$ than ND-AspRS (K_D value of 2.1 µM, Figure 1B). These divergent K_D values differ from those obtained using the *T. thermophilus* partners, where $tRNA^{Asn}$ bound to ND-AspRS with higher affinity than to GatCAB (21). The asymmetric K_D values determined with the *H. pylori* system were confirmed by DLS (Figure 2). Indeed, a higher-sized particle was clearly seen in the presence of ND-AspRS and $tRNA^{Asp}$ (12.6 nm), compared to free ND-AspRS and tRNA (10.9 and 4.9 nm, respectively) but not when ND-AspRS and $tRNA^{Asn}$ were mixed (Figure 2, lanes 1–4) (10.9 nm). Similarly, we detected an association between GatCAB and $tRNA^{Asn}$ (10.9 nm) compared to their isolated counterparts (9.4 and 4.9 nm, respectively) (Figure 2, lanes 5 and 6). No association of the protein partners in the absence of tRNA was detected by either technique (data not shown). Finally, when the three partners were mixed, a new ribonucleoprotein (RNP) of significantly higher size (13.5 nm) appeared (Figure 2, lane 7). Isolation of this complex by gel-filtration (Figure 1C) and analysis of its components by SDS–PAGE (Figure 1D) revealed the presence of ND-AspRS, the three GatCAB subunits and $tRNA^{Asn}$. Functional analysis confirmed that it was fully able to synthesize Asn-$tRNA^{Asn}$ in the presence of free Asp, ATP and Gln (Figure 1E). Because the association of the protein partners is $tRNA^{Asn}$-dependent, this complex constitutes a *bona fide* Asn-transamidosome according to previous arguments (21).

Dynamics of the *H. pylori* Asn-transamidosome

In *T. thermophilus*, the Asn-transamidosome is characterized by its remarkable stability in gel filtration (21,22), whereas for *H. pylori*, it is less stable (Figure 1C). Since this observation could reflect a difference in dynamic properties, we tested the stability of the *Hp* Asn-transamidosome by measuring its hydrodynamic

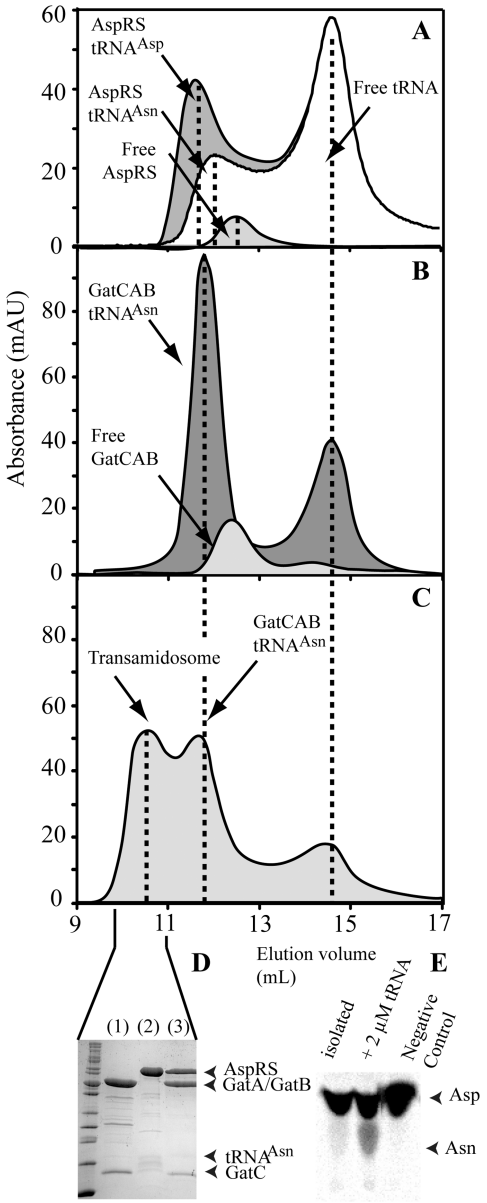

Figure 1. Size-exclusion chromatography shows formation of a transamidosome complex by ND-AspRS, GatCAB and $tRNA^{Asn}$. (**A**) Comparison of isolated ND-AspRS and ND-AspRS/$tRNA^{Asp}$ and ND-AspRS/$tRNA^{Asn}$ complexes. The observed association enabled an estimation of the K_D value for binding of each tRNA to ND-AspRS (see 'Materials and Methods' section). K_D values for the binding to ND-AspRS are 7.9 and 21.4 μM for $tRNA^{Asp}$ and $tRNA^{Asn}$, respectively. (**B**) Comparison between free GatCAB and GatCAB/$tRNA^{Asn}$ complexes. The K_D value for this association is 2.1 μM. (**C**) Elution profile of a mixture containing GatCAB, ND-AspRS and $tRNA^{Asn}$. (**D**) SDS–PAGE profile of a SEC fraction (lane 3) compared to GatCAB alone (lane 1) and ND-AspRS alone (lane 2). (**E**) TLC plate demonstrating that the complex eluted in the first peak (termed 'isolated') is able to produce Asn-$tRNA^{Asn}$ alone, or when supplemented with excess $tRNA^{Asn}$ (termed '+2 μM tRNA'), compared to a negative control where GatCAB was omitted. All partners were mixed to a final concentration of 20 μM each. All K_D values determined varied within 10%.

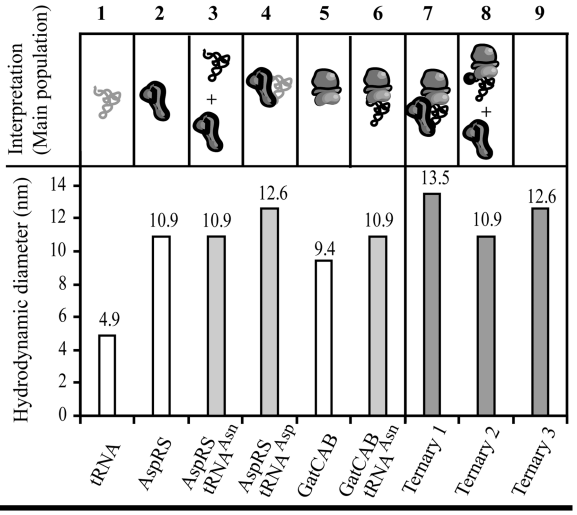

	1	2	3	4	5	6	7	8	9
AspRS (μM)	-	20	20	20	-	-	20	20	20
GatCAB (μM)	-	-	-	-	20	20	20	20	20
$tRNA^{Asp}$ (μM)	40	-	-	20	-	-	-	-	-
$tRNA^{Asn}$ (μM)	-	-	20	-	-	20	20	20	20
L-Asp (mM)	-	-	-	-	-	-	-	2	2
ATP (mM)	-	-	-	-	-	-	-	2	2
L-Gln (mM)	-	-	-	-	-	-	-	-	2
Apparent mass (kD)	27	178	178	250	126	178	294	178	250
Real mass (kD)	25	131	131	181	113	138	400	131	181

Figure 2. Characterization of the complexes involving *Hp* ND-AspRS, GatCAB, $tRNA^{Asn}$ and $tRNA^{Asp}$ by DLS and analysis of the stability of the transamidosome under catalytic and non-catalytic conditions. Each value is an average of five independent measurements with errors <5%. All the experiments were conducted under the same conditions as size chromatography experiments (see 'Materials and Methods' section). Ternary 1, 2 and 3 all refer to the transamidosome under non-catalytic (1), aspartylation (2) and aspartylation/transamidation (3) conditions.

diameter in the presence of small substrates, e.g. under catalytic conditions. The particle size decreased from 13.6 nm under non-catalytic conditions to 10.9 nm under aspartylation conditions (i.e. presence of Asp and ATP), and from 13.6 to 12.9 nm under transamidation conditions (i.e. presence of Asp, ATP and Gln). Furthermore, gel-filtration with a mix of GatCAB, ND-AspRS and preformed Asp-$tRNA^{Asn}$ revealed elution of the binary GatCAB/Asp-$tRNA^{Asn}$ complex and a separate ND-AspRS peak (data not shown). These results suggest that charging of $tRNA^{Asn}$ may trigger destabilization of the transamidosome (Figure 2, lanes 7–9), apparently through release of ND-AspRS. Hence the *Hp* Asn-transamidosome displays completely different dynamics than does its *T. thermophilus* counterpart (21).

Helicobacter pylori ND-AspRS, an enzyme with dual kinetic behavior

Table 1 summarizes the steady-state kinetic parameters of *Hp* ND-AspRS for aminoacylation of $tRNA^{Asp}$ and

Table 1. Kinetic constants for aspartylation of $tRNA^{Asp}$ and $tRNA^{Asn}$ and a tRNA variant with *H. pylori* ND-AspRS in the absence and presence of GatCAB

	−GatCAB		Burst	+GatCAB	
	k_{cat} (s^{-1})	K_M (μM)		k_{cat} (s^{-1})	K_M (μM)
$tRNA^{Asp}$	0.33 ± 0.01	n.d.	−	0.31	n.d.
$tRNA^{Asn}$	0.14 ± 0.02	0.08 ± 0.01	+	0.25 ± 0.03	0.3 ± 0.03
yeast $tRNA^{Asp}$	0.29 ± 0.03	n.d.	−	n.d.	n.d.
$tRNA^{Asn}$ (G_1–C_{72}, U_{20A})	0.26 ± 0.02	n.d.	+	0.28 ± 0.02	n.d.

Burst indicates the presence of an initial fast phase of tRNA aminoacylation.

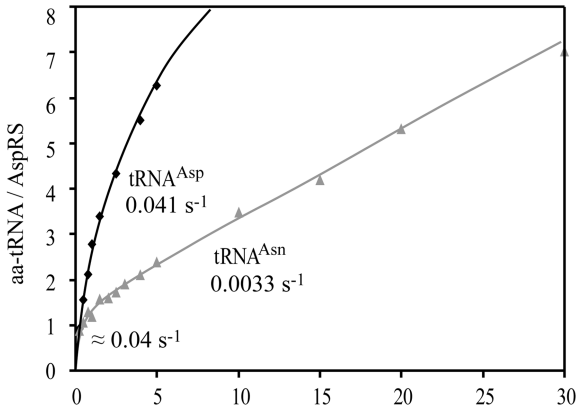

Figure 3. Aminoacylation kinetics for $tRNA^{Asp}$ and $tRNA^{Asn}$ with *Hp* ND-AspRS: a dual response to substrates. Experiments were conducted in 15% glycerol at 4°C for $tRNA^{Asp}$ (black diamonds) and $tRNA^{Asn}$ (gray triangles). Results show that $tRNA^{Asp}$ and $tRNA^{Asn}$ are aminoacylated differently. In case of $tRNA^{Asp}$, the first cycle (1 Asp-tRNA formed) has the same rate as the subsequent ones ($0.04\,s^{-1}$). However, in case of $tRNA^{Asn}$, the first cycle ($0.04\,s^{-1}$), which is equivalent to that for $tRNA^{Asp}$, is significantly faster than the subsequent ones ($0.0033\,s^{-1}$). Extrapolation of this slower phase at t_0 points to the formation of 1 Asp-$tRNA^{Asn}$ per ND-AspRS active site. This pattern suggests a rate-limiting step which would be the release of Asp-$tRNA^{Asn}$. SE was <5% on all values.

$tRNA^{Asn}$. The enzyme aspartylates $tRNA^{Asp}$ 2.5-fold faster than $tRNA^{Asn}$ (0.33 and $0.14\,s^{-1}$), as reported previously (32). However, pre-steady-state kinetics conducted under conditions that allowed an examination of the first catalytic cycles of the enzyme (4°C and in the presence of 10 or 15% of glycerol) revealed intriguing differences in aminoacylation of both tRNAs since in contrast to $tRNA^{Asp}$ the charging kinetics of $tRNA^{Asn}$ were biphasic. Aminoacylation of $tRNA^{Asp}$ remains linear after completion of the first catalytic cycle. Thus, this first cycle occurs with the same rate as subsequent ones ($0.041\,s^{-1}$) (Figure 3). Since ATP-PPi exchange rate is significantly faster than tRNA charging (15.9 and $0.33\,s^{-1}$ at 37°C), the steady-state rate of $tRNA^{Asp}$ aminoacylation is dictated by the rate of transfer of activated Asp onto $tRNA^{Asp}$. Surprisingly, when $tRNA^{Asn}$ is used as a substrate, biphasic kinetics arise, which exhibit a burst of Asp-$tRNA^{Asn}$ formation ($\sim 0.04\,s^{-1}$) followed by a significantly slower linear phase ($0.0033\,s^{-1}$) (Figure 3). Extrapolation of the linear phase at t_0 points to formation of one Asp-$tRNA^{Asn}$ per ND-AspRS active site during the fast phase (Figure 3) and suggests that the first $tRNA^{Asn}$ is aspartylated significantly faster than those following. Interestingly, the first $tRNA^{Asn}$ is aminoacylated with a rate equivalent to that observed for $tRNA^{Asp}$ (Figure 3). Burst and steady-state rate values are both dependent on enzyme concentration (Supplementary Figure S1A). In the slow phase, the steady-state rate of $tRNA^{Asn}$ charging increases with the pH but not significantly with the ionic strength (Supplementary Figure S1B). This kinetic behavior is consistent with the release of Asp-$tRNA^{Asn}$ being the rate-limiting step at the steady-state of the reaction (40). The slow dissociation of the Asp-$tRNA^{Asn}$ product agrees with the absence of detectable hydrolysis of its ester bond in the presence of ND-AspRS (28).

GatCAB modifies the kinetic properties for $tRNA^{Asn}$

Table 1 shows the effect of GatCAB on kinetic constants of *Hp* ND-AspRS for $tRNA^{Asn}$ and $tRNA^{Asp}$ aspartylation. The addition of GatCAB increases the steady-state rate of Asp-$tRNA^{Asn}$ formation according to a hyperbolic curve (Figure 4A), but has no effect on the steady-state rate of $tRNA^{Asp}$ charging (Figure 4A, inset and Table 1), indicating that this phenomenon is specific to $tRNA^{Asn}$. When saturating concentrations of GatCAB are reached, the rate of $tRNA^{Asn}$ aspartylation increases 1.8-fold ($0.14–0.25\,s^{-1}$) and nearly fits that of $tRNA^{Asp}$ ($0.33\,s^{-1}$, Table 1), while the K_M value of ND-AspRS for $tRNA^{Asn}$ increases 3.8-fold, leading to an increase in the overall charging efficiency (k_{cat}/K_M) of 1.8-fold (Table 1). Thus, in the presence of GatCAB, aminoacylation of $tRNA^{Asn}$ occurs with a similar efficiency as that of $tRNA^{Asp}$ (k_{cat}/K_M, respectively of 0.27 and $0.30\,\mu M^{-1}\,s^{-1}$). Pre-steady-state kinetics reveal that this GatCAB-mediated effect originates in an increase in the rate of aminoacylation during the slow phase ($0.0033–0.012\,s^{-1}$, Figure 5A and B). The rate of the fast phase does not seem to be affected (Figure 5B). Considering that $tRNA^{Asn}$ binds GatCAB and ND-AspRS with K_D values of 2.1 and 21.4 μM, respectively (Figure 1), and that aspartylation of $tRNA^{Asn}$ is more efficient when it is 'labeled' with or 'presented' by GatCAB (Table 1), the GatCAB/$tRNA^{Asn}$ complex may constitute a better substrate for misacylation by the ND-AspRS. We named this complex the $tRNA^{Asn}$-presentation complex (tRNPC). Since this complex is non-productive in absence of ND-AspRS and can also be a substrate, tRNPC can be considered as a *bona fide* transfer ribonucleoprotein (tRNP).

Interestingly, the tRNPC has opposing effects on the discriminating AspRS of *E. coli* (D-AspRS) (Figure 4B) *in vitro*. *Ec* D-AspRS is able to aspartylate $tRNA^{Asn}$, in addition to its cognate $tRNA^{Asp}$, albeit much less efficiently (14). As shown for other mischarging kinetics of non-cognate tRNAs, the transfer step is rate-limiting (41). GatCAB decreases the rate of aminoacylation of $tRNA^{Asn}$ by the D-AspRS (Figure 5B). This result can be

interpreted through the strong binding of $tRNA^{Asn}$ on GatCAB and the low affinity of the D-AspRS for $tRNA^{Asn}$. In contrast to the *H. pylori* system, GatCAB decreases the rate of Asp-$tRNA^{Asn}$ formation by *Ec* D-AspRS presumably through sequestration of $tRNA^{Asn}$ limiting the free $tRNA^{Asn}$ available for aminoacylation. Thus, the enhancing effect of GatCAB is restricted to $tRNA^{Asn}$ aspartylation by ND-AspRS.

In vivo experiments confirmed that expression of *Hp* ND-AspRS in the transformed *E. coli* ER Asn-auxotrophic strain was toxic presumably because of the accumulation of Asp-$tRNA^{Asn}$ (Supplementary Figure S2), as previously shown (32). An antibiogram-like test with an IPTG-soaked paper disk clearly triggers a growth defect phenotype compared to controls (Supplementary Figure S2A–C). Co-expression of *Hp* GatCAB reduces this toxic effect, since the enzyme is able to convert Asp-$tRNA^{Asn}$ into Asn-$tRNA^{Asn}$ allowing growth of the recombined strain (Supplementary Figure S2D), although with lesser efficiency.

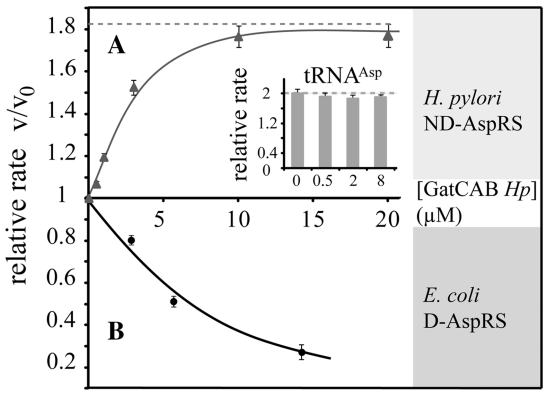

Figure 4. Effects of GatCAB on aminoacylation of $tRNA^{Asn}$ using *Hp* ND-AspRS versus *Ec* D-AspRS. The graph shows the effect of increasing GatCAB concentrations on initial rates of both AspRSs in the presence of saturating $tRNA^{Asn}$ concentration. Results (v) were normalized using the steady-state rate value of the corresponding AspRS in absence of GatCAB (v_0). Concentration of the GatCAB/$tRNA^{Asn}$ complex increases together with GatCAB concentration. (**A**) GatCAB increases the steady-state rate of *Hp* ND-AspRS when $tRNA^{Asn}$ is present (gray triangles), but not when $tRNA^{Asp}$ is used (*inset*). Error bars represent the SD from three independent experiments. (**B**) GatCAB decreases the steady-state rate of $tRNA^{Asn}$ misacylation with *Ec* D-AspRS.

GatCAB helps to release Asp-$tRNA^{Asn}$ from the ND-AspRS active site

The acceleration of the steady-state rate of $tRNA^{Asn}$ aspartylation by GatCAB (Figure 5) suggests that GatCAB controls the release of Asp-$tRNA^{Asn}$ from the ND-AspRS active site. To test this hypothesis, we used a strategy to nullify this effect without altering GatCAB or ND-AspRS. In other words, we asked whether this effect was solely due to the ability of GatCAB to bind Asp-$tRNA^{Asn}$. To this end, we investigated aspartylation of $tRNA^{Asn}$ variant mutated at positions known to determine recognition by GatCAB (38). The U_1–A_{72} base-pair constitutes the major transamidation determinant, but recognition of $tRNA^{Asn}$ is further favored by the absence of the U_{20A} position in the D-loop (38). Importantly, these positions are not critical for ND-AspRS recognition (38,42). Thus, we constructed a G_1–C_{72}:U_{20A}-containing $tRNA^{Asn}$ variant and verified that it is a suitable substrate for ND-AspRS but is not recognized by GatCAB (Figure 6 and 38). The aminoacylation kinetics of this $tRNA^{Asn}$ variant remained biphasic and saturating levels of GatCAB had no effect on the steady-state rate of aminoacylation (Figure 6A and B). Thus, removing the ability of GatCAB to bind this mutant Asp-$tRNA^{Asn}$ eliminated the impact of GatCAB on ND-AspRS kinetics. These results indicate that GatCAB enhances ND-AspRS kinetics by recognizing the wild-type aspartylated extremity of $tRNA^{Asn}$ according to the transamidation determinants, consequently freeing the ND-AspRS active site. As a

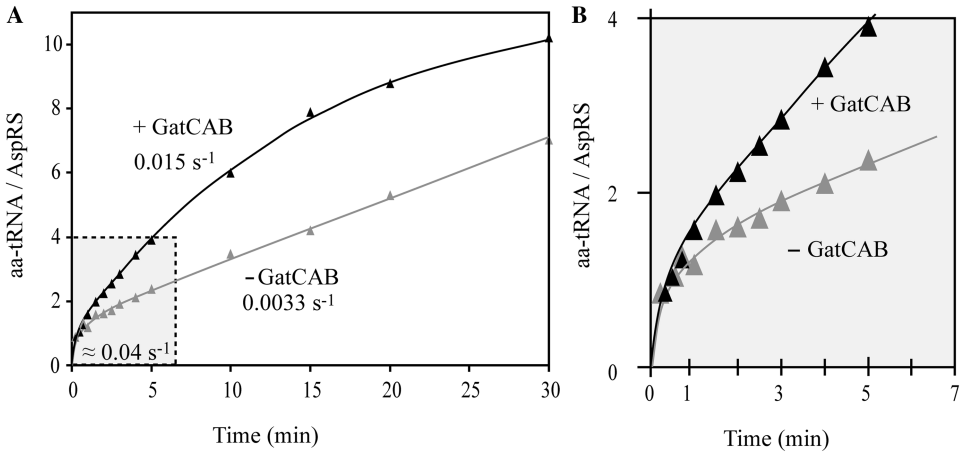

Figure 5. GatCAB influences aminoacylation kinetics for $tRNA^{Asn}$ with *Hp* ND-AspRS. Pre-steady-state kinetics were conducted under the same conditions of pre-steady-state as previously (4°C, 15% glycerol). (**A**) In the presence of saturating GatCAB concentration (10 μM), the steady-state rate of $tRNA^{Asn}$ misacylation increases and the burst value slightly decreases. These results suggest that GatCAB increases the dissociation of Asp-$tRNA^{Asn}$. (**B**) Zoom on the 4 first aminoacylation cycles (in the presence of GatCAB), corresponding to the gray zone in (A). SE was <5% on all values.

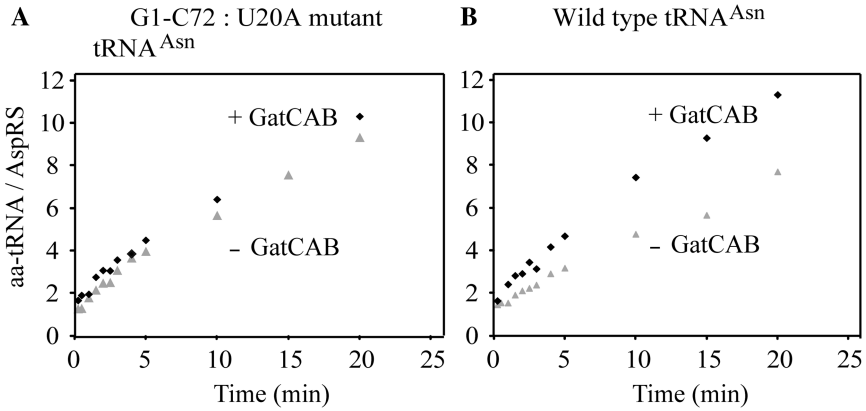

Figure 6. GatCAB pulls Asp-tRNA^{Asn} from the ND-AspRS active site. (**A**) Pre-steady-state kinetics performed with a tRNA^{Asn} mutated at the GatCAB identity elements: G_1–C_{72}:U_{20A} replace the natural U_1–A_{72}:Δ_{20A} positions. Addition of GatCAB (black diamonds, +GatCAB) has no effect on the steady-state rate, compared to a reaction without GatCAB (gray triangles, −GatCAB). (**B**) Pre-steady-state kinetics performed with a wild-type tRNA^{Asn}. Addition of GatCAB (black diamonds, +GatCAB) accelerates the steady-state rate, compared to a reaction without GatCAB (gray triangles, −GatCAB).

consequence, the overall turnover of ND-AspRS increases in the presence of GatCAB.

Origin of the rate-limiting step

What are the structural elements that trigger different aminoacylation mechanisms with respect to tRNA^{Asp} and tRNA^{Asn}? The major differences between bacterial tRNA^{Asp} and tRNA^{Asn} lie within the acceptor arm (displaying a G_1–C_{72} or a U_1–A_{72} base pair, respectively) and the anticodon loop (positions C_{36} and U_{36} and C_{38} and A_{38} in tRNA^{Asp} and tRNA^{Asn}, respectively). Yeast cytoplasmic tRNA^{Asp} provides a natural variant that displays a GUC 'Asp' anticodon and a bacterial 'tRNA^{Asn}-like' acceptor-end that almost avoids aminoacylation by *Ec* D-AspRS (43). Similar to bacterial tRNA^{Asp}, aminoacylation of yeast tRNA^{Asp} is monophasic (data not shown). Thus, the elements leading to the biphasic kinetics for aminoacylation of tRNA^{Asn} by the *Hp* ND-AspRS are absent in yeast tRNA^{Asp}. Further, substitution of C_{36} by U_{36} in bacterial tRNA^{Asp} leading to a GUU 'Asn' anticodon did not trigger a biphasic kinetic response (data not shown). Hence, the divergent kinetic responses of *Hp* ND-AspRS for tRNA^{Asp} versus tRNA^{Asn} aminoacylation are probably triggered by different overall conformations of the aminoacyl-tRNA end-products, rather than by distinct affinities for the tRNA substrates. This hypothesis is in line with the fact that the two k_{cat}'s of aspartylation (Table 1) show opposing trends with respect to the affinities of the enzyme for the two tRNAs (Figure 1). Moreover, the steady-state rate of tRNA^{Asn} aspartylation is more affected by increase of the pH than by that of the ionic strength (Supplementary Figure S1), suggesting that the aminoacylated tRNA^{Asn} extremity, and mostly the Asp moiety, plays a prevalent role in the slow dissociation of Asp-tRNA^{Asn}, in accordance with other studies on the rate-limiting step of tRNA aminoacylation (40) and the inhibition properties of Asp-ol-AMP. Interestingly, this non-hydrolyzable Asp-AMP mimic, competitive with respect to Asp and ATP, shows different inhibition patterns for aminoacylation of tRNA^{Asp} and tRNA^{Asn} (39 and Supplementary Table S1). Indeed K_i values of 8 and 32 μM were determined in presence of tRNA^{Asp} and tRNA^{Asn}, respectively (Supplementary Table S1). This 4-fold increase in the K_i value when Asp-tRNA^{Asn} is formed suggests a strong binding of the tRNA^{Asn}-bound Asp moiety within ND-AspRS active site, compared to Asp-tRNA^{Asp}. This is further confirmed with differential inhibition patterns using Asp-ol-AMP (Supplementary Table S1) in presence of tRNAAsp or tRNAAsn, the latter tRNA protecting the active site from inhibition more efficiently as a consequence of its retention. This is in agreement with a previous work on *Pseudomonas aeruginosa* ND-AspRS (39) showing that the limiting step for Asp-tRNAAsn synthesis could be general for ND-AspRS of bacterial type.

To obtain further insights into the origin of the distinct dissociation rates of the two aminoacyl-tRNAs from ND-AspRS, we performed Arrhenius activation energy (E_A) measurements (Supplementary Figure S3). The E_A values are the same for aminoacylation of tRNA^{Asp} ($68.6 \pm 0.6\,kJmol^{-1}K^{-1}$) and tRNA^{Asn} ($66.9 \pm 1.9\,kJmol^{-1}K^{-1}$). Thus, both E_A are determined by the same step, presumably the transfer step, since the release of aminoacyl-tRNA does not contribute significantly to E_A. From these similar E_A values, one can suggest that the steps preceding the release of Asp-tRNA are equivalent and that the differences occur after the transfer step. It is therefore reasonable to assume that the formation of Asp-tRNA^{Asp}, or Asp-tRNA^{Asn} trigger different structural arrangements of the active site. This conformational difference may explain the difference in Asp-tRNA release and in inhibition patterns by Asp-ol AMP.

DISCUSSION

The Asn-transamidosome in *H. pylori*

Previous work has suggested that an Asn-transamidosome should exist in *H. pylori* (28). Indeed, this organism does

not import Asn (44), and given the fact that no Asn synthetase or AsnRS could be detected in the genome using BLAST, the indirect misacylation/transamidation pathway seems to be the sole route for Asn and Asn-tRNA^{Asn} biosynthesis, as is also the case for Gln-tRNA^{Gln} (24). *Hp* ND-AspRS and GatCAB participate together with tRNA^{Asn} in the formation of a ribonucleoprotein homologous to that shown for *T. thermophilus* (Figures 1 and 2). Contrary to the *T. thermophilus* Asn-transamidosome (21), we noticed that, in the *Hp* system, uncharged tRNA^{Asn} has a 10-fold stronger affinity for GatCAB (the second enzyme of the pathway) than for ND-AspRS (the first enzyme in the pathway) (Figures 1 and 2). Thus, in *H. pylori*, ND-AspRS presumably docks onto the tRNPC, rather than to free tRNA^{Asn} (Scheme 1). In conditions where GatCAB is in excess, tRNA^{Asn} may thus be mostly presented by GatCAB, ensuring the proper channeling of Asp-tRNA^{Asn} toward GatCAB. Consistently, the tRNPC seems to be a better substrate for aminoacylation than free tRNA^{Asn} (Table 1 and Figure 4). Upon aspartylation, the Asp-tRNA^{Asn} acceptor-end shifts toward the GatCAB active site and triggers the release of ND-AspRS from the complex (Figure 2, lanes 7–9), explaining why the steady-state rate of ND-AspRS increases in the transamidosome. Indeed, when GatCAB is present, Asp-tRNA^{Asn} gets pulled out of the ND-AspRS active site, freeing ND-AspRS from its product and allowing a new catalytic cycle to occur as evidenced by the faster steady-state rate of aspartylation.

This scheme strongly differs from that determined for the *T. thermophilus* Asn-transamidosome, where the complex remains stable over the entire catalytic cycle, according to a peculiar flip-flop mechanism involving a non-substrate scaffold tRNA ($_{scaf}$tRNA) (22). Indeed, *Tt* ND-AspRS, unlike *Hp* ND-AspRS, changes its release mode and retains Asp-tRNA^{Asn}, to preserve the tRNP stability when GatCAB is present, e.g. within the complex. These major differences in stability and in mechanism could be due to the differences between *Tt* and *Hp* ND-AspRSs. Indeed, while *Tt* ND-AspRS belongs to the archaeal structural-type, *Hp* ND-AspRS falls into the bacterial structural-type which contains an additional domain, called the GAD domain. This domain is appended to the active site where it could prevent the scaffold tRNA from playing its role, or it could destabilize the overall complex (22). Either of these effects would result in lesser stability and greater dynamics for the bacterial-type Asn-transamidosome. On the other hand, while *Tt* ND-AspRS does not retain its Asp-tRNA^{Asn} product in the absence of GatCAB (22) (i.e. outside the complex), *Hp* ND-AspRS might be able to trap this aminoacyl-tRNA thanks to the GAD domain, which lies next to the active site in a position where an editing domain is found in the class II homologous ThrRS (45)

ND-AspRS displays a dual mode of release for its two Asp-tRNA products

ND-AspRS recognizes and aspartylates both tRNA^{Asp} and tRNA^{Asn} equivalently, which makes it a ND enzyme for substrate recognition and aminoacylation. Nevertheless, kinetic studies clearly show a difference in product release. Asp-tRNA^{Asn} is retained upon aminoacylation, while Asp-tRNA^{Asp} is not (Figure 3). This difference seems to be triggered by the overall conformation of tRNA rather than by specific identity elements. Our results suggest that the shapes of tRNA^{Asp} and tRNA^{Asn} could induce different active site configurations that lead to these divergent modes of release. According to the predominant effect of pH on the steady-state rate (slower phase) (Supplementary Figure S1), the CCA-Asp moiety may play an important role in Asp-tRNA^{Asn} retention on ND-AspRS. This is further confirmed with differential inhibition patterns using Asp-ol-AMP (Supplementary Table S1) in presence of tRNA^{Asp} or tRNA^{Asn}, the latter tRNA protecting the active site from inhibition more efficiently as a consequence of its retention. This is in agreement with a previous work on *P. aeruginosa* ND-AspRS (39) showing that the limiting step for Asp-tRNA^{Asn} synthesis could be general for ND-AspRS of bacterial type.

This scheme strongly shares analogy with editing mechanisms, where a tRNA gets misacylated with a wrong or near-cognate amino acid and retained on the enzyme to be edited. However, here, a cognate amino acid is loaded onto a 'non-cognate' tRNA^{Asn} and the Asp-tRNA^{Asn} product gets retained, perhaps to statistically favor further processing of the misacylated intermediate by GatCAB prior to its release (Scheme 1). We named this a 'rescue mechanism'; it may be essential under conditions where GatCAB is not found in sufficient amounts within the cell or when it is occupied in the glutaminylation pathway that also exists in *H. pylori*.

Taking into account the hypothesis forged from a kinetic study (8), the rate-limiting step of ND-AspRS, like all class II aaRSs, is expected to be the transfer of activated Asp onto tRNA. In contrast, in class I aaRSs, the rate-limiting step is typically product release. Clearly, *Hp* ND-AspRS shifts to a class I-like kinetic behavior with tRNA^{Asn} but retains its class II character with tRNA^{Asp}. Previously, it has been demonstrated that the class II phosphoseryl-tRNA synthetase (SepRS) used in the Cys-tRNA^{Cys} biosynthesis indirect pathway in *Methanocaldococcus janaschii*, also has a rate-limiting step for the release of the aminoacyl-tRNA (46). The authors hypothesized that this characteristic could have evolved from modifications of the motifs implicated in aminoacylation, accelerating the transfer step over release, leading to a new rate-limiting step compared to other class II enzymes that is more similar to class I. ND-AspRS is a new example of an aaRS that can shift from a class II to a class I-like kinetic behavior, according to its tRNA substrate. This phenomenon fully correlates with the fates of Asp-tRNA products, since Asp-tRNA^{Asn} should be retained on ND-AspRS until GatCAB transforms it into Asn-tRNA^{Asn}, while Asp-tRNA^{Asp} should be released in line with its 'cognate' status. Together, these results allow us to make an analogy between the misacylation/transamidation pathway and editing strategies encountered with several classical aaRSs.

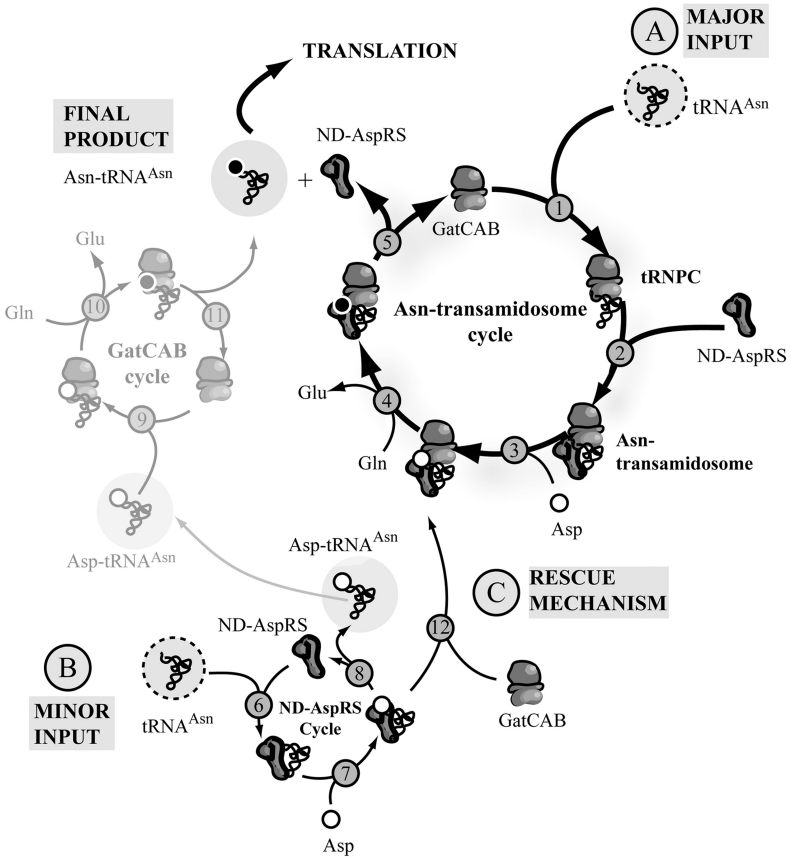

Step	Name	Constants			
1	Binding of tRNA on GatCAB Formation of the tRNPC	K_D = 2.1 µM	–	Asn-transamidosome cycle	A
2	Binding of ND-AspRS onto the tRNPC : formation of the Asn-transamidosome	–	–		
3	Aspartylation of $tRNA^{Asn}$	K_M = 0.3 µM	k_{cat} = 0.33 s^{-1}		
4	Transamidation of Asp-$tRNA^{Asn}$	K_M = 1.12 µM	k_{cat} = 0.25 s^{-1}		
5	Release of Asn-$tRNA^{Asn}$ and ND-AspRS	–	–		
6	Binding of $tRNA^{Asn}$ on ND-AspRS	K_D = 21.4 µM		ND-AspRS cycle	B
7	Aspartylation of $tRNA^{Asn}$	K_M = 0.08 µM	k_{cat} = 0.14 s^{-1}		
8	Dissociation of Asp-$tRNA^{Asn}$ from ND-AspRS	–	–		
9	Association of Asp-$tRNA^{Asn}$ to GatCAB	–	–	GatCAB cycle	
10	Transamidation of Asp-$tRNA^{Asn}$	K_M = 2.1 µM	k_{cat} = 0.25 s^{-1}		
11	Release of Asn-$tRNA^{Asn}$ from GatCAB	–	–		
12	Binding of GatCAB on Asp-$tRNA^{Asn}$/ND-AspRS complex : **Rescue mechanism (R.M)**	–	–	R.M	C

Scheme 1. Formation of Asn-$tRNA^{Asn}$ in *H. pylori*. (**A**) The major pathway used in *H. pylori* (the main 'Asn-transamidosome pathway') starts with (1) the formation of the tRNPC, linking GatCAB and $tRNA^{Asn}$, onto which (2) ND-AspRS can then dock to form the Asn-transamidosome. In this ribonucleoprotein, $tRNA^{Asn}$ gets aspartylated more efficiently (3), and the aspartylated CCA-end of $tRNA^{Asn}$ shifts from the ND-AspRS active site to the GatCAB phosphorylation/amidation active site. Asn-$tRNA^{Asn}$ biosynthesis proceeds thanks to amide donor hydrolysis (here free Gln) to provide the ammonia moiety necessary for transamidation (4) (28). When Asn-$tRNA^{Asn}$ is formed, it is released together with ND-AspRS, and used in protein synthesis (5). (**B**) When GatCAB is not in sufficient amounts to produce enough tRNPC, free $tRNA^{Asn}$ binds to ND-AspRS (6) and gets aminoacylated less efficiently (7). The dissociation of Asp-$tRNA^{Asn}$ is rate-limiting, but if Asp-$tRNA^{Asn}$ is released (8), GatCAB can still recognize it (9) and transamidate it (10) (28) into Asn-$tRNA^{Asn}$, which can be released to fuel translation (11). (**C**) Since the release of Asp-$tRNA^{Asn}$ from ND-AspRS is rate-limiting, Asp-$tRNA^{Asn}$ remains within the ND-AspRS active site for longer times, enabling free GatCAB to bind to the ND-AspRS/Asp-$tRNA^{Asn}$ complex (12) to form an Asn-transamidosome, in which Asn-$tRNA^{Asn}$ can be synthesized through transamidation (4) rejoining the main Asn-transamidosome cycle. This latter mechanism can be qualified as a 'rescue mechanism'. The table summarizes the different pathway characteristics. The aspartylation and transamidation steps are highlighted to stress the fact that the Asn-transamidosome pathway couples both reactions, while they are sequential when GatCAB is absent or when the tRNPC is not involved.

Transamidosomes are editing-like systems that enlarged the genetic code

AaRSs are responsible for matching a tRNA and its cognate amino acid. Many of these enzymes acquired catalytic peculiarities that nowadays ensure homologous aminoacyl-tRNA production, with an error rate compatible with survival of the cell (4,47,48). In spite of their specificity, aaRSs are known to use non-cognate amino acid or metabolic precursors to form mischarged aminoacyl-tRNAs. ValRS and IleRS can respectively produce Thr-tRNA^{Val} and Val-tRNA^{Ile} (49,50), and LeuRS can misacylate isoleucine, methionine, homocysteine, α-amino butyrate and norvaline onto tRNA^{Leu} (51). The release of mischarged aminoacyl-tRNA is normally prevented by correction mechanisms [either hydrolysis of the non-cognate aminoacyl∼AMP intermediate (pre-transfer editing) or hydrolysis of the ester linkage of the mischarged aminoacyl-tRNA (post-transfer editing)] (4,49–53). Post-transfer correction is thought to rely on aminoacyl-tRNA dissociation as the rate-limiting step providing time for the misacylated aminoacyl-tRNA acceptor arm to shift from the active site to the editing site. Interestingly, this mechanism completely relies on the presence of the cognate tRNA (54). Post-transfer editing can also be achieved by autonomous trans-editing factors (4). Indeed, as an example, ProRS and tRNA^{Pro} form a stable complex together with YbaK to avoid accumulation of Cys-tRNA^{Pro} and subsequent mistranslation (55).

Asn and Gln-transamidosomes constitute an assembly of an ND-aaRS (ND-AspRS or ND-GluRS/GluRS2), a 'non-cognate' tRNA (tRNA^{Asn} or tRNA^{Gln}) and a homeotopic modification enzyme (56); together these components ensure accurate synthesis of the cognate aminoacyl-tRNA pair. Since they reduce toxicity of misacylated species by preventing their release into the cellular medium, Asn- and Gln-transamidosomes could also be considered as kinetic systems related to editing systems that increase the faithfulness of aminoacylation and protect the integrity of the genetic code (Supplementary Figure S2 and 21,24). In *H. pylori*, the Asn-transamidosome mimics a post-transfer editing system, in which GatCAB would play a role similar to a trans-editing factor, except that the misacylated aminoacyl-tRNA does not get hydrolyzed but is rather modified into a cognate aminoacyl-tRNA. In line with this scenario, it is noteworthy that indirect pathways are thought to be ancient routes that allowed ancient 'Asp' and 'Glu' codons to be shifted into 'Asn' and 'Gln' codons and could thus be regarded as codon reassignment systems (24). Indeed, before GatCAB appeared, tRNA^{Asn} and tRNA^{Gln} were considered as normal ND-AspRS and GluRS substrates. However, among past Asp-tRNAs, the present-day tRNA^{Asn} emerged with a different kinetic behavior that favored its modification by GatCAB. While editing systems restricted and still restrict the combinations of small molecules that can be linked to tRNAs, Asn and Gln-transamidosomes were ribonucleoprotein systems that enlarged the genetic code by shifting some Asp-tRNA and Glu-tRNA species into Asn-tRNA^{Asn} and Gln-tRNA^{Gln}.

GatCAB is a node for transamidation

Helicobacter pylori belongs to a subclass of organisms that lack both GlnRS and AsnRS, in which GatCAB plays a dual role in glutaminylation and asparaginylation. In contrast, archaea possess two tRNA-dependent amidotransferases each specific for one pathway (57). In *H. pylori*, GatCAB is able to bind very efficiently to uncharged tRNA^{Asn} (this study) but also to tRNA^{Gln} (24) with equivalent affinities (2.1 and 2.0 μM, respectively) (Supplementary Scheme S1). This capacity provides two types of tRNA-presentation complexes: tRNPC and the tRNA^{Gln}-presentation complex (tRQPC), which may represent a way to target GatCAB toward ND-AspRS and asparaginylation on one hand and GluRS2 (the enzyme specific for tRNA^{Gln} misacylation in *Hp*) (25,34) and glutaminylation on the other hand (Supplementary Scheme S1). This need to share GatCAB between two distinct aaRSs could explain the reason why the Asn- and Gln-transamidosomes are both more dynamic in *H. pylori* than in *T. thermophilus* (22) or *T. maritima* (23). Hence, transamidosomes may be adapted to the metabolic context and physiology of the organism from which they originate.

SUPPLEMENTARY DATA

Supplementary Data are available at NAR Online: Supplementary Table 1, Supplementary Scheme 1 and Supplementary Figures 1–3.

ACKNOWLEDGEMENTS

We thank Prof. E. Westhof and Dr R. Giegé (IBMC) for support, Prof. R. Chênevert (Université Laval, Québec) for providing Asp-ol-AMP and M. Brayé (IBMC) for technical assistance.

FUNDING

Natural Sciences and Engineering Research Council of Canada (9597-2010 to J.L.); Fond de Recherche sur la Nature et les Technologies du Québec (PR-105093 to J.L., Robert Chênevert and Paul H. Roy, and graduate fellowship to J.L.H.); Regroupement Québecois de Recherche sur la Fonction, la Structure et l'Ingénierie des Proteines (PROTEO) (graduate fellowship to J.L.H.); 'Ministère du Développement Économique, de l'Innovation et de l'Exportation (MDEIE) du Québec' [grant PSR-SIIRI-095/ESFARN to J.L., Sheng-Xiang Lin and Robert Chênevert, in collaboration with Prof. You-Xin Jin at the Shanghai Institute of Biological Sciences (SIBS), Chinese Academy of Sciences]; Ministère de l'Education Nationale, de la Recherche et de la Technologie (graduate fellowship to F.F.); Université de Strasbourg, Centre National de la Recherche Scientifique and Association pour la Recherche sur le Cancer (to D.K.) and National Institutes of Health (R01GM071480 to T.L.H.). Funding for open access charge: Centre National de la Recherche

Scientifique, Université de Strasbourg, Association de la Recherche sur le Cancer.

Conflict of interest statement. None declared.

REFERENCES

1. Kern,D. and Lapointe,J. (1979) The twenty aminoacyl-tRNA synthetases from *Escherichia coli*. General separation procedure, and comparison of the influence of pH and divalent cations on their catalytic activities. *Biochimie*, **61**, 1257–1272.
2. Kern,D., Dietrich,A., Fasiolo,F., Renaud,M., Giegé,R. and Ebel,J.P. (1977) The yeast aminoacyl-tRNA synthetases. Methodology for their complete or partial purification and comparison of their relative activities under various extraction conditions. *Biochimie*, **59**, 453–462.
3. Jakubowsky,H. (2005) Accuracy of aminoacyl-tRNA synthetases: proofreading of amino acids. In: Ibba,M., Francklyn,C. and Cusack,S. (eds), *The Aminoacyl-tRNA Synthetases*. Landes Bioscience, Georgetown, TX, pp. 384–396.
4. Ling,J., Reynolds,N. and Ibba,M. (2009) Aminoacyl-tRNA synthesis and translational quality control. *Annu. Rev. Microbiol.*, **63**, 61–78.
5. Eriani,G., Delarue,M., Poch,O., Gangloff,J. and Moras,D. (1990) Partition of tRNA synthetases into two classes based on mutually exclusive sets of sequence motifs. *Nature*, **347**, 203–206.
6. Fraser,T.H. and Rich,A. (1975) Amino acids are not all initially attached to the same position on transfer RNA molecules. *Proc. Natl Acad. Sci. USA*, **72**, 3044–3048.
7. Sprinzl,M. and Cramer,F. (1975) Site of aminoacylation of tRNAs from *Escherichia coli* with respect to the 2′- or 3′-hydroxyl group of the terminal adenosine. *Proc. Natl Acad. Sci. USA*, **72**, 3049–3053.
8. Zhang,C.M., Perona,J.J., Ryu,K., Francklyn,C. and Hou,Y.M. (2006) Distinct kinetic mechanisms of the two classes of aminoacyl-tRNA synthetases. *J. Mol. Biol.*, **361**, 300–311.
9. Kern,D., Roy,H. and Becker,H.D. (2005) Asparaginyl-tRNA synthetases. In: Ibba,M., Francklyn,C. and Cusack,S. (eds), *The Aminoacyl-tRNA Synthetases*. Landes Bioscience, Georgetown, TX, pp. 193–209.
10. Feng,L., Tumbula-Hansen,D., Min,B., Namgoong,S., Salazar,J., Orellana,O. and Söll,D. (2005) Transfer-RNA-dependent amidotransferases: key enzymes for Asn-tRNA^{Asn} and Gln-tRNA^{Gln} synthesis in nature. In: Ibba,M., Francklyn,C. and Cusack,S. (eds), *The Aminoacyl-tRNA Synthetases*. Landes Bioscience, Georgetown, TX, pp. 193–209.
11. Martin,R.P., Schneller,J.M., Stahl,A.J. and Dirheimer,G. (1977) Study of yeast mitochondrial tRNAs by two-dimensional polyacrylamide gel electrophoresis. Characterization of isoaccepting species and search for imported cytoplasmic tRNAs. *Nucleic Acids Res.*, **4**, 3497–3510.
12. Wilcox,M. and Nirenberg,M. (1968) Transfer RNA as a cofactor coupling amino acid synthesis with that of protein. *Proc. Natl Acad. Sci. USA.*, **61**, 229–236.
13. Curnow,A.W., Hong,K., Yuan,R., Kim,S., Martins,O., Winkler,W., Henkin,T.M. and Söll,D. (1997) Glu-tRNA^{Gln} amidotransferase: a novel heterotrimeric enzyme required for correct decoding of glutamine codons during translation. *Proc. Natl Acad. Sci. USA*, **94**, 11819–11826.
14. Becker,H.D. and Kern,D. (1998) *Thermus thermophilus*: a link in evolution of the tRNA-dependent amino acid amidation pathways. *Proc. Natl Acad. Sci. USA*, **95**, 12832–12837.
15. Curnow,A.W., Tumbula,D.L., Pelaschier,J.T., Min,B. and Söll,D. (1998) Glutamyl-tRNA^{Gln} amidotransferase in *Deinococcus radiodurans* may be confined to asparagine biosynthesis. *Proc. Natl Acad. Sci. USA*, **95**, 12838–12843.
16. Schön,A., Kannangara,C.G., Gough,S. and Söll,D. (1988) Protein biosynthesis in organelles requires misaminoacylation of tRNA. *Nature*, **331**, 187–190.
17. Curnow,A.W. and Söll,D. (1996) tRNA-dependent asparagine formation. *Nature*, **382**, 589–590.
18. Pujol,C., Bailly,M., Kern,D., Maréchal-Drouard,L., Becker,H. and Duchêne,A.M. (2008) Dual-targeted tRNA-dependent amidotransferase ensures both mitochondrial and chloroplastic Gln-tRNA^{Gln} synthesis in plants. *Proc. Natl Acad. Sci. USA*, **105**, 6481–6485.
19. Frechin,M., Senger,B., Brayé,M., Kern,D., Martin,R.P. and Becker,H.D. (2009) Yeast mitochondrial Gln-tRNA^{Gln} is generated by a GatFAB-mediated transamidation pathway involving Arc1p-controlled subcellular sorting of cytosolic GluRS. *Genes Dev.*, **23**, 1119–1130.
20. Sheppard,K., Yuan,J., Hohn,M.J., Jester,B., Devine,K.M. and Söll,D. (2008) From one amino acid to another: tRNA-dependent amino acid biosynthesis. *Nucleic Acids Res.*, **36**, 1813–1825.
21. Bailly,M., Blaise,M., Lorber,B., Becker,H.D. and Kern,D. (2007) The transamidosome: a dynamic ribonucleoprotein particle dedicated to prokaryotic tRNA-dependent asparagine biosynthesis. *Mol. Cell*, **28**, 228–239.
22. Blaise,M., Bailly,M., Frechin,M., Behrens,M.A., Fischer,F., Oliveira,C.L., Becker,H.D., Pedersen,J.S., Thirup,S. and Kern,D. (2010) Crystal structure of a transfer-ribonucleoprotein particle that promotes asparagine formation. *EMBO J.*, **29**, 3118–3129.
23. Ito,T. and Yokoyama,S. (2010) Two enzymes bound to one transfer RNA assume alternative conformations for consecutive reactions. *Nature*, **467**, 612–616.
24. Huot,J.L., Fischer,F., Corbeil,J., Madore,E., Lorber,B., Diss,G., Hendrickson,T.L., Kern,D. and Lapointe,J. (2011) Gln-tRNA^{Gln} synthesis in a dynamic transamidosome from *Helicobacter pylori*, where GluRS2 hydrolyzes excess Glu-tRNA^{Gln}. *Nucleic Acids Res.*, **39**, 9306–9315.
25. Salazar,J.C., Ahel,I., Orellana,O., Tumbula-Hansen,D., Krieger,R., Daniels,L. and Söll,D. (2003) Coevolution of an aminoacyl-tRNA synthetase with its tRNA substrates. *Proc. Natl. Acad. Sci. USA*, **100**, 13863–13868.
26. Chang,K.M. and Hendrickson,T.L. (2009) Recognition of tRNA^{Gln} by *Helicobacter pylori* GluRS2 a tRNA^{Gln}-specific glutamyl-tRNA synthetase. *Nucleic Acids Res.*, **37**, 6942–6949.
27. Sheppard,K., Akochy,P.M., Salazar,J.C. and Söll,D. (2007) The *Helicobacter pylori* amidotransferase GatCAB is equally efficient in glutamine-dependent transamidation of Asp-tRNA^{Asn} and Glu-tRNA^{Gln}. *J. Biol. Chem.*, **282**, 11866–11873.
28. Huot,J.L., Balg,C., Jahn,D., Moser,J., Emond,A., Blais,S.P., Chênevert,R. and Lapointe,J. (2007) Mechanism of a GatCAB amidotransferase: aspartyl-tRNA synthetase increases its affinity for Asp-tRNA^{Asn} and novel aminoacyl-tRNA analogues are competitive inhibitors. *Biochemistry*, **46**, 13190–13198.
29. Stanzel,M., Schön,A. and Sprinzl,M. (1994) Discrimination against misacylated tRNA by chloroplast elongation factor Tu. *Eur. J. Biochem.*, **219**, 435–439.
30. Roy,H., Becker,H.D., Mazauric,M.H. and Kern,D. (2007) Structural elements defining elongation factor Tu mediated suppression of codon ambiguity. *Nucleic Acids Res.*, **35**, 3420–3430.
31. Ruan,B., Palioura,S., Sabina,J., Marvin-Guy,L., Kochhar,S., Larossa,R.A. and Söll,D. (2008) Quality control despite mistranslation caused by an ambiguous genetic code. *Proc. Natl. Acad. Sci. USA*, **105**, 16502–16507.
32. Chuawong,P. and Hendrickson,T.L. (2006) The nondiscriminating aspartyl-tRNA synthetase from *Helicobacter pylori*: anticodon-binding domain mutations that impact tRNA specificity and heterologous toxicity. *Biochemistry*, **45**, 8079–8087.
33. Nüñez,H., Lefimil,C., Min,B., Söll,D. and Orellana,O. (2004) *In vivo* formation of glutamyl-tRNA^{Gln} in *Escherichia coli* by heterologous glutamyl-tRNA synthetases. *FEBS Lett.*, **557**, 133–135.
34. Skouloubris,S., Ribas de Pouplana,L., De Reuse,H. and Hendrickson,T.L. (2003) A non cognate aminoacyl-tRNA synthetase that may resolve a missing link in protein evolution. *Proc. Natl. Acad. Sci. USA*, **100**, 11297–11302.
35. Pelchat,M., Lacoste,L., Yang,F. and Lapointe,J. (1998) Overproduction of the *Bacillus subtilis* glutamyl-tRNA synthetase in its host and its toxicity to *Escherichia coli*. *Can. J. Microbiol.*, **44**, 378–381.
36. Barros,M.H., Rak,M., Paulela,J.A. and Tzagaloff,A. (2011) Characterization of Gtf1p, the connector subunit of yeast

mitochondrial tRNA-dependent amidotransferase. *J. Biol. Chem.*, **286**, 32937–32947.
37. Martin,F., Eriani,G., Eiler,S., Moras,D., Dirheimer,G. and Gangloff,J. (1993) Overproduction and purification of native and queuine-lacking *Escherichia coli* $tRNA^{Asp}$. Role of the wobble base in $tRNA^{Asp}$ acylation. *J. Mol. Biol.*, **234**, 965–974.
38. Bailly,M., Giannouli,S., Blaise,M., Stathopoulos,C., Kern,D. and Becker,H.D. (2006) A single tRNA base-pair mediates bacterial tRNA-dependent biosynthesis of asparagine. *Nucleic Acids Res.*, **34**, 6083–6094.
39. Bernard,D., Akochy,P.M., Bernier,S., Fisette,O., Brousseau,O.C., Chênevert,R., Roy,P.H. and Lapointe,J. (2007) Inhibition by L-aspartol adenylate of a nondiscriminating aspartyl-tRNA synthetase reveals differences between the interactions of its active site with $tRNA^{Asp}$ and $tRNA^{Asn}$. *J. Enzyme Inhib. Med. Chem.*, **22**, 77–82.
40. Kern,D. and Gangloff,J. (1981) Catalytic mechanism of valyl-tRNA synthetase from baker's yeast. Reaction pathway and rate-determining step in the aminoacylation of $tRNA^{Val}$. *Biochemistry*, **20**, 2065–2074.
41. Kern,D. (1981) Aminoacyl-tRNA synthétases. Etudes structurales et fonctionnelles. *Thèse d'État*. Université Louis Pasteur Strasbourg.
42. Giegé,R., Florentz,C., Kern,D., Gangloff,J., Eriani,G. and Moras,D. (1996) Aspartate identity of transfer RNAs. *Biochimie*, **78**, 605–623.
43. Moulinier,L., Eiler,S., Eriani,G., Gangloff,J., Thierry,J.C., Gabriel,K., McClain,W.H. and Moras,D. (2001) The structure of an AspRS-$tRNA^{Asp}$ complex reveals a tRNA-dependent control mechanism. *EMBO J.*, **20**, 5290–5301.
44. Leduc,D., Gallaud,J., Stingl,K. and de Reuse,H. (2010) Coupled amino acid deamidase-transport systems essential for *Helicobacter pylori* colonization. *Infect. Immun.*, **78**, 2782–2792.
45. Sankaranarayanan,R., Dock-Bregeon,A.C., Romby,P., Caillet,J., Springer,M., Rees,B., Ehresmann,C., Ehresmann,B. and Moras,D. (1999) The structure of threonyl-tRNA synthetase-$tRNA^{Thr}$ complex enlightens its repressor activity and reveals an essential zinc ion in the active site. *Cell*, **97**, 371–381.
46. Zhang,C.M., Liu,C., Slater,S. and Hou,Y.M. (2008) Aminoacylation of tRNA with phosphoserine for synthesis of cysteinyl-$tRNA^{Cys}$. *Nat. Struct. Mol. Biol.*, **15**, 507–514.
47. Loftfield,R.B. and Vanderjagdt,D. (1972) The frequency of errors in protein biosynthesis. *Biochem. J.*, **128**, 1353–1356.
48. Reynolds,N.M., Lazazzera,B.A. and Ibba,M. (2010) Cellular mechanisms that control mistranslation. *Nat. Rev. Microbiol.*, **8**, 849–856.
49. Fersht,A. (1978) Editing mechanisms in the aminoacylation of tRNA, in transfer RNA: structure properties and recognition. In: Schimmel,P.R., Söll,D. and Abelson,J.N. (eds), Cold Spring Harbor, USA, pp. 247–254.
50. Cramer,F., Von der Haar,F. and Igloi,G.L. (1978) Mechanism of aminoacyl-tRNA synthetases: recognition and proofreading processes. In: Schimmel,P.R., Söll,D. and Abelson,J.N. (eds), *Transfer RNA: Structure Properties and Recognition*. Cold Spring Harbor, USA, pp. 267–279.
51. Tan,M., Zhu,B., Zhou,X.L., He,R., Chen,X., Eriani,G. and Wang,E.D. (2010) tRNA-dependent pre-transfer editing by prokaryotic leucyl-tRNA synthetase. *J. Biol. Chem.*, **285**, 3235–3244.
52. Igloi,G.L., Von der Haar,F. and Cramer,F. (1977) Hydrolytic action of aminoacyl-tRNA synthetases from baker's yeast: chemical proofreading of Thr-$tRNA^{Val}$ by valyl-tRNA synthetase studied with modified $tRNA^{Val}$ and amino acid analogues. *Biochemistry*, **16**, 1696–1702.
53. Eldred,E.W. and Schimmel,P.R. (1972) Rapid deacylation by isoleucyl-transfer ribonucleic acid synthetase of isoleucine-specific transfer ribonucleic acid aminoacylated with valine. *J. Biol. Chem.*, **247**, 2961–2964.
54. Bonnet,J. and Ebel,J.P. (1974) Correction of aminoacylation errors: evidence for a non significant role of the aminoacyl-tRNA synthetase catalysed deacylation of aminoacyl-tRNAs. *FEBS Lett.*, **39**, 259–262.
55. An,S. and Musier-Forsyth,K. (2005) Cys-$tRNA^{Pro}$ editing by *Haemophilus influenzae* YbaK via a novel synthetase.YbaK.tRNA ternary complex. *J. Biol. Chem.*, **280**, 34465–34472.
56. Danchin,A. (1989) Homeotopic transformation and the origin of translation. *Prog. Biophys. Mol. Biol.*, **54**, 81–86.
57. Sheppard,K., Sherrer,R.L. and Söll,D. (2008) *Methanothermobacter thermautotrophicus* $tRNA^{Gln}$ confines the amidotransferase GatCAB to asparaginyl-$tRNA^{Asn}$ formation. *J. Mol. Biol.*, **377**, 845–853.